EURASIP Journal on
Wireless Communications and Networking
a SpringerOpen Journal

RESEARCH Open Access

Optimal pilot symbol power allocation under time-variant channels

Michal Šimko[1*], Qi Wang[1] and Markus Rupp[1]

Abstract

Nowadays, most wireless communication systems employ coherent demodulation on the receiver side. Under this circumstance, part of the available transmission resource is reserved and utilized for channel estimation, referred to as pilot symbols. In recent standards, for example long-term evolution (LTE), a certain adjustment is allowed for the power radiated on the pilot symbols. This additional degree of freedom creates space for a further optimization of the system performance. In this article, we consider an orthogonal frequency division multiplexing system and investigate how to distribute the available power between data symbols and pilot symbols under transmissions over time-variant channels so that the overall throughput is maximized. We choose the post-equalization signal-to-interference and noise ratio as the cost function and solve the problem analytically. Simulation results obtained by the Vienna LTE simulator are consistent with the analytical results. With an optimal power distribution between data and pilot symbols, a throughput increase of around 10% can be achieved compared to a system with evenly distributed power between data and pilot symbols.

Introduction

Nowadays, most wireless communication systems are based on orthogonal frequency division multiplexing (OFDM), for example worldwide inter-operability for microwave access (WiMAX) and long-term evolution (LTE). At the receiver side, coherent detection is employed where channel estimation is required. For the purpose of channel estimation, known symbols are inserted into the transmitted data stream. These so-called pilot symbols consume available resources like bandwidth and power. Some standards, e.g., LTE, allow to assign different power levels to the data and pilot subcarriers, which makes room for system optimization. A power increase at the pilot subcarriers results in a more reliable channel estimate [1] which implies higher throughput; however, the power available for the data subcarriers is decreased given a constant sum power constraint. Therefore, it is necessary to find an optimal power allocation between the pilot and data subcarriers which delivers a maximized system performance.

In the meanwhile, high mobility users are considered to be supported by standardization organizations due to the increasing demand of high-speed data connections on the move. LTE, for example, aims to serve users moving up to 500 km/h. At such velocities, the aforementioned power distribution problem becomes even more challenging, mainly because of two reasons:

1. In Section "Channel estimation" ahead, we show that the channel estimation error becomes saturated with the increasing Doppler spread. Therefore, a power boost at the pilots does not necessary lead to a better channel estimate.
2. A high Doppler spread destroys the desired orthogonality between subcarriers. The system performance becomes limited by the simple and low-cost channel estimation based on individual subcarriers. Therefore, a more sophisticated channel estimation scheme is required.

Related study

In order to optimize the pilot symbol power allocation under time-varying channels, a model that takes into account the pilot power adjustment, receiver structure, and channel estimation error at the same time, is needed. It has been shown by simulation that the channel capacity strongly depends on the power that is assigned to the pilot symbols [2]. Authors of [3] showed the impact of different

*Correspondence: msimko@nt.tuwien.ac.at
[1] Institute of Telecommunications, Vienna University of Technology, Vienna, Austria

power allocations on the bit error ratio (BER). However, their analysis was based on the signal-to-noise ratio (SNR); only an approximation of the impact of imperfect channel knowledge on BER was provided for a simple binary phase-shift keying modulation. In [4], an optimal pilot symbol allocation was derived analytically for phase-shift keying modulation of order two and four, using BER as the optimization criterion. In [5], the optimal pilot symbol power in multiple input multiple output (MIMO) systems was derived based on a lower bound for capacity. Authors of [6] investigated power allocations between pilot and data symbols for MIMO systems using the post-equalization signal-to-interference and noise ratio (SINR) as an optimization function. However, they only approximated the SINR expression; only a linear minimum mean square error (LMMSE) channel estimator was considered.

In [1], the authors derived the optimal power distribution between pilot and data symbols for time-invariant channels under imperfect channel knowledge. The optimal distribution of power turned out to be independent of the SNR and channel realizations. In [7], this study was extended to multi eNodeB scenarios where the interference from neighboring eNodeBs was included. Due to the LTE pilot symbol design, the pilot symbols from neighboring eNodeBs are overlapping with the data symbols in the eNodeB of interest, which complicates the optimization problem.

Contribution

In this article, we consider zero forcing (ZF) equalizers under imperfect channel knowledge in a time-variant scenario and develop an analytical model for the post-equalization SINR. In order to answer the question, how to distribute the available power between data and pilot symbols, we choose the post-equalization SINR as the cost function which implies a maximization of the system throughput. Contributions of this article are:

- We deliver an optimal pilot symbol power adjustment in MIMO OFDM systems under time-variant channels.
- A post-equalization SINR expression is derived for a ZF receiver under realistic, imperfect channel knowledge.
- The analytical derivation of mean squared error (MSE) performance is provided for least squares (LS) channel estimators utilizing a two-dimensional linear interpolation in the time-frequency grid.
- Simulation results with an LTE compliant simulator [8,9] confirm our theoretical analysis.[a]

The remainder of the article is organized as follows. In the following section, we introduce a mathematical model for MIMO OFDM transmissions. In Section "Post-equalization SINR", we derive the post-equalization SINR expression for ZF equalizers with imperfect channel knowledge. The channel estimators that are involved in this study as well as their MSEs are briefly discussed in Section "Channel estimation". In Section "Power allocation", we formulate the optimization problem for optimal pilot symbol power allocation. Finally, we present LTE simulation results in Section "Simulation results" and conclude the article in Section "Conclusion".

Transmission model

In this section, we briefly point out the key aspects in the LTE standard that are relevant to this article and introduce a transmission model suitable for our further derivation. The most important variables used in this article and their description are summarized in Table 1.

In the time domain, the LTE signal consists of frames with a duration of 10 ms. Each frame is split into ten equally long subframes and each subframe into two equally long slots with a duration of 0.5 ms. With the normal cyclic prefix length, each slot consists of $N_\mathrm{s} = 7$ OFDM symbols; with the extended cyclic prefix length, $N_\mathrm{s} = 6$. In LTE, the subcarrier spacing is fixed to 15 kHz. Twelve adjacent subcarriers in one slot are grouped into a so-called resource block. The number of resource blocks in an LTE slot ranges from 6 up to 100, corresponding to a bandwidth from 1.4 up to 20 MHz. Figure 1 displays the pilot symbol pattern in LTE. The colored squares correspond to pilot symbols. If there is a pilot symbol inserted on a specific position in the time-frequency grid at one transmit antenna, the remaining antennas on that position remain silent. In Figure 1, crosses correspond to these silent positions. Such pilot symbol pattern allows to estimate a MIMO channel as multiple, individual single input single output (SISO) channels as long as the spatial correlation is neglected.

A received OFDM symbol in the frequency domain at the n_rth receive antenna can be written as

$$\tilde{\mathbf{y}}_{n_\mathrm{r}} = \sum_{n_\mathrm{t}=1}^{N_\mathrm{t}} \tilde{\mathbf{H}}_{n_\mathrm{t},n_\mathrm{r}} \mathbf{x}_{n_\mathrm{t}} + \tilde{\mathbf{n}}_{n_\mathrm{r}}, \tag{1}$$

where $\tilde{\mathbf{H}}_{n_\mathrm{t},n_\mathrm{r}} \in \mathbb{C}^{N_\mathrm{sub} \times N_\mathrm{sub}}$ represents the channel matrix in the frequency domain between the n_tth transmit and n_rth receive antennas. The transmitted signal vector is referred to as $\mathbf{x}_{n_\mathrm{t}}$, the received signal vector as $\tilde{\mathbf{y}}_{n_\mathrm{r}}$. The vector $\tilde{\mathbf{n}}_{n_\mathrm{r}} \in \mathbb{C}^{N_\mathrm{sub} \times 1}$ is additive white zero mean Gaussian noise with variance σ_n^2 on antenna n_r. In case of a time-invariant channel, the channel matrix $\tilde{\mathbf{H}}_{n_\mathrm{t},n_\mathrm{r}}$ appears as a diagonal matrix, whereas a time-variant channel forces the channel matrix $\tilde{\mathbf{H}}_{n_\mathrm{t},n_\mathrm{r}}$ to become non-diagonal. These non-diagonal elements indicate that the subcarriers are not orthogonal anymore, leading to the so-called intercarrier interference (ICI).

Table 1 Most important variables

Variable	Dimension	Description
$\tilde{\mathbf{y}}_{n_r}$	$\mathbb{C}^{N_{\text{sub}}\times 1}$	Received symbol vector at antenna n_r
$\tilde{\mathbf{H}}_{n_r,n_t}$	$\mathbb{C}^{N_{\text{sub}}\times N_{\text{sub}}}$	Channel matrix between antennas n_t and n_r in frequency domain
x_{n_t}	$\mathbb{C}^{N_{\text{sub}}\times 1}$	Transmit symbol vector at antenna n_t
$\mathbf{x}_{\text{p},n_t}$	$\mathbb{P}^{N_p\times 1}$	Pilot symbols vector at antenna n_t
$\mathbf{x}_{\text{d},n_t}$	$\mathbb{C}^{N_d\times 1}$	Transmit data vector at antenna n_t
$\tilde{\mathbf{n}}_{n_r}$	$\mathbb{C}^{N_{\text{sub}}\times 1}$	Additive noise at antenna n_r
$\mathbf{y}_k$	$\mathbb{C}^{N_r\times 1}$	Received symbol vector at subcarrier k
$\mathbf{H}_{k,l}$	$\mathbb{C}^{N_r\times N_t}$	Channel matrix between subcarriers k and l
$\mathbf{W}_k$	$\mathbb{C}^{N_t\times N_l}$	Precoding matrix at subcarrier k
$\mathbf{G}_{k,k}$	$\mathbb{C}^{N_r\times N_l}$	Effective channel matrix $\mathbf{H}_{k,k}\mathbf{W}_k$
$\mathbf{s}_k$	$\mathbb{D}^{N_l\times 1}$	Transmit data at subcarrier k
$\mathbf{n}_k$	$\mathbb{C}^{N_r\times 1}$	Additive noise at subcarrier k
$\mathbf{E}_k$	$\mathbb{C}^{N_r\times N_t}$	Channel estimation error at subcarrier k
σ_s^2	$\mathbb{R}$	Transmit power of one layer
σ_{p}^2	$\mathbb{R}$	Transmit pilot symbol power
σ_x^2	$\mathbb{R}$	Transmit data power
σ_{ICI}^2	$\mathbb{R}$	ICI power
σ_n^2	$\mathbb{R}$	Noise power
σ_e^2	$\mathbb{R}$	Channel estimation error variance
d	$\mathbb{R}$	Channel saturation coefficient
f_c	$\mathbb{R}$	Carrier frequency
$v_{\max}$	$\mathbb{R}$	Maximal user velocity
f_d	$\mathbb{R}$	Maximal Doppler frequency
T_s	$\mathbb{R}$	OFDM symbol duration
N_{p}	$\mathbb{N}$	Number of pilot symbols
N_{d}	$\mathbb{N}$	Number of data symbols
N_{l}	$\mathbb{N}$	Number of layers
N_{t}	$\mathbb{N}$	Number of transmit antennas
N_{r}	$\mathbb{N}$	Number of receive antennas
N_{sub}	$\mathbb{N}$	Number of subcarriers
p_{off}	$\mathbb{R}$	Offset between power of pilot symbols and data symbols
γ_l	$\mathbb{R}$	Post-equalization SINR at layer l

Specifically, the vector $\mathbf{x}_{n_t} \in \mathbb{C}^{N_{\text{sub}}\times 1}$ in Equation (1) comprises the precoded data symbols $\mathbf{x}_{\text{d},n_t} \in \mathbb{C}^{N_d\times 1}$ and the pilot symbols $\mathbf{x}_{\text{p},n_t} \in \mathbb{P}^{N_p\times 1}$ from the set of all possible pilot symbols $\mathbb{P}$ defined in LTE, at the n_tth transmit antenna placed by a suitable permutation matrix $\mathbf{P}$

$$\mathbf{x}_{n_t} = \mathbf{P}\left[\mathbf{x}_{\text{p},n_t}^{\text{T}}\ \mathbf{x}_{\text{d},n_t}^{\text{T}}\right]^{\text{T}}. \tag{2}$$

The vector $\mathbf{x}_{n_t}$ has N_{sub} entries, corresponding to the number of non-zero subcarriers. Let us denote the number of pilot symbols and the number of precoded data symbols by N_{p} and N_{d}, respectively. On subcarrier k of the data symbol vector $\mathbf{x}_{\text{d},n_t}$, the precoding process can be described as

$$\left[x_{\text{d},1,k}\cdots x_{\text{d},N_t,k}\right]^{\text{T}} = \mathbf{W}_k\left[s_{1,k}s_{2,k}\cdots s_{N_l,k}\right]^{\text{T}}, \tag{3}$$

where $x_{\text{d},n_t,k}$ is a precoded data symbol at the n_tth transmit antenna port and the kth subcarrier, $\mathbf{W}_k \in \mathbb{C}^{N_t\times N_l}$ is a unitary precoding matrix at the kth subcarrier and $s_{n_l,k} \in \mathbb{D}^{1\times 1}$ is the data symbol of the n_lth layer at the kth subcarrier. Here, $\mathbb{D}$ is the set of available modulation alphabets. In LTE, three different sets can be used, namely 4 quadrature amplitude modulation (QAM), 16 QAM, and 64 QAM. In order to obtain data symbol vectors $\mathbf{x}_{\text{d},n_t}$, one has to stack data symbols $x_{\text{d},n_t,k}$ obtained via Equation (3) at a specific antenna n_t into a vector.

For the derivation of the post-equalization SINR, we will use a MIMO input–output relation at the subcarrier level, given as:

$$\mathbf{y}_k = \mathbf{H}_{k,k}\mathbf{W}_k\mathbf{s}_k + \mathbf{n}_k + \underbrace{\sum_{m\neq k}\mathbf{H}_{k,m}\mathbf{W}_m\mathbf{s}_m}_{\text{ICI}}. \tag{4}$$

Matrix $\mathbf{H}_{k,m} \in \mathbb{C}^{N_r\times N_t}$ denotes the MIMO channel matrix between the kth and mth subcarriers. The MIMO channel matrix $\mathbf{H}_{k,m}$ contains appropriately ordered elements of matrices $\tilde{\mathbf{H}}_{n_t,n_r}$ located in the kth row and mth column. Matrix $\mathbf{W}_k$ is a unitary precoding matrix of size $N_t\times N_l$. In LTE, the precoding matrix can be chosen from a finite set of precoding matrices [10]. The vector $\mathbf{s}_k$ consists of the data symbols of all layers at the kth subcarrier. Vector $\mathbf{n}_k$ represents additive white zero mean Gaussian noise with variance σ_n^2 at subcarrier k. We denote the effective channel matrix by

$$\mathbf{G}_{k,k} = \mathbf{H}_{k,k}\mathbf{W}_k. \tag{5}$$

Furthermore, the average power transmitted on each of the N_l layers is denoted by σ_s^2. The total power transmitted on one data position is σ_{d}^2, while that on one pilot position is σ_{p}^2.

Example. When the power is evenly distributed between the data and pilot symbols, there is:

$$\sigma_s^2 = \mathbb{E}\left\{\|s_{l,k}\|_2^2\right\} = \frac{1}{N_l}, \tag{6}$$

$$\sigma_{\text{d}}^2 = \frac{1}{N_{\text{d}}}\sum_{n_t=1}^{N_t}\mathbb{E}\left\{\|\mathbf{x}_{\text{d},n_t}\|_2^2\right\} = 1, \tag{7}$$

$$\sigma_{\text{p}}^2 = \frac{1}{N_{\text{p}}}\sum_{n_t=1}^{N_t}\mathbb{E}\left\{\|\mathbf{x}_{\text{p},n_t}\|_2^2\right\} = 1, \tag{8}$$

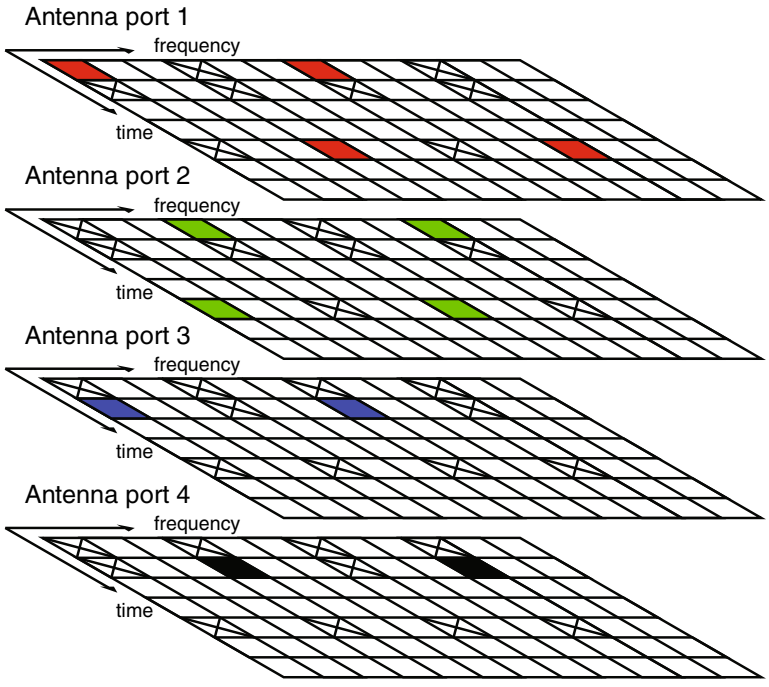

Figure 1 Pilot symbol pattern utilized in LTE over time and frequency for four antennas. Colored squares represent pilot symbols and the crossed squares silent symbols.

where N_{d} is the number of data symbols and N_{p} the number of pilot symbols.

Post-equalization SINR

In this section, we consider a time-variant scenario and derive an analytical expression for the post-equalization SINR of a MIMO system using a ZF equalizer based on imperfect channel knowledge.

If perfect channel knowledge available at the equalizer, the ZF estimate of the data symbol $\mathbf{s}_k$ is given as

$$\hat{\mathbf{s}}_k = \left(\mathbf{G}_{k,k}^{\mathrm{H}}\mathbf{G}_{k,k}\right)^{-1}\mathbf{G}_{k,k}^{\mathrm{H}}\mathbf{y}_k. \tag{9}$$

The data estimate $\hat{\mathbf{s}}_k$ given by Equation (9) results in a post-equalization SINR of the lth layer given as [11]

$$\gamma_l = \frac{\sigma_s^2}{\left(\sigma_n^2 + \sigma_{\mathrm{ICI}}^2\right)\mathbf{e}_l^{\mathrm{H}}\left(\mathbf{G}_{k,k}^{\mathrm{H}}\mathbf{G}_{k,k}\right)^{-1}\mathbf{e}_l}, \tag{10}$$

where the vector $\mathbf{e}_l$ is an $N_{\mathrm{l}} \times 1$ zero vector with a one on the lth element. This vector extracts the signal on the corresponding layer after the equalizer. The variable σ_{ICI}^2 represents the ICI power, that is given as

$$\sigma_{\mathrm{ICI}}^2 = \mathbb{E}\left\{\sum_{m\neq k}\|\mathbf{H}_{k,m}\mathbf{W}_m\mathbf{s}_m\|_2^2\right\}. \tag{11}$$

Authors of [12] derived the ICI power leaking from neighboring subcarriers due to the loss of orthogonality between subcarriers. For a typical assumption of the Jake's spectrum, the ICI power σ_{ICI}^2 can be expressed as

$$\sigma_{\mathrm{ICI}}^2 = 1 - \int_{-1}^{1}(1-|x|)\,\mathrm{J}_0\left(2\pi f_d T_s x\right)dx, \tag{12}$$

where $\mathrm{J}_0(\cdot)$ denotes the zeroth-order Bessel function, representing the channel time autocorrelation function. Variable f_{d} represents the maximal Doppler frequency and T_{s} the OFDM symbol duration. The maximal Doppler frequency can be obtained by the following expression

$$f_{\mathrm{d}} = \frac{v_{\max} f_c}{c_0}, \tag{13}$$

where $v_{\max}$ is the maximal user velocity, f_{c} the carrier frequency, and c_0 the speed of light.Let us proceed to the case of imperfect channel knowledge. We define the perfect channel as the channel estimate plus the error matrix due to the imperfect channel estimation

$$\mathbf{H}_{k,k} = \hat{\mathbf{H}}_{k,k} + \mathbf{E}_{k,k}, \tag{14}$$

where the elements of the matrix $\mathbf{E}_{k,k}$ are random variables, statistically independent of each other, each with variance σ_e^2. Inserting Equation (14) in Equation (4), the input–output relation changes to

$$\mathbf{y}_k = \left(\hat{\mathbf{H}}_{k,k} + \mathbf{E}_{k,k}\right)\mathbf{W}_k\mathbf{s}_k + \mathbf{n}_k + \sum_{m\neq k}\mathbf{H}_{k,m}\mathbf{W}_m\mathbf{s}_m. \tag{15}$$

Since the channel estimation error matrix $\mathbf{E}_{k,k}$ is unknown at the receiver, the ZF solution is given again by Equation (9), but channel matrix $\mathbf{H}_{k,k}$ is replaced by its estimate $\hat{\mathbf{H}}_{k,k}$, which is known at the receiver

$$\hat{\mathbf{s}}_k = \left(\hat{\mathbf{G}}_{k,k}^{\mathrm{H}} \hat{\mathbf{G}}_{k,k}\right)^{-1} \hat{\mathbf{G}}_{k,k}^{\mathrm{H}} \mathbf{y}_k, \tag{16}$$

with matrix $\hat{\mathbf{G}}_{k,k}$ being equal to $\hat{\mathbf{H}}_{k,k}\mathbf{W}_k$. The symbol error after the ZF equalizer is given as

$$\hat{\mathbf{s}}_k - \mathbf{s}_k = \left(\hat{\mathbf{G}}_{k,k}^{\mathrm{H}} \hat{\mathbf{G}}_{k,k}\right)^{-1} \hat{\mathbf{G}}_{k,k}^{\mathrm{H}} \times \left(\mathbf{E}_{k,k}\mathbf{W}_k\mathbf{s}_k + \mathbf{n}_k + \sum_{m \neq k} \mathbf{H}_{k,m}\mathbf{W}_m\mathbf{s}_m\right). \tag{17}$$

From Equation (17), we can compute the MSE matrix assuming that the estimation error matrix and the effective channel matrix are statistically independent

$$\begin{aligned} \mathrm{MSE} &= \mathbb{E}\left\{\left(\hat{\mathbf{s}}_k - \mathbf{s}_k\right)\left(\hat{\mathbf{s}}_k - \mathbf{s}_k\right)^{\mathrm{H}}\right\} \\ &= \left(\sigma_n^2 + \sigma_{\mathrm{ICI}}^2 + \sigma_{\mathrm{d}}^2\sigma_e^2\right)\left(\hat{\mathbf{G}}_{k,k}^{\mathrm{H}} \hat{\mathbf{G}}_{k,k}\right)^{-1}, \end{aligned} \tag{18}$$

with σ_e^2 being the MSE of the channel estimator. Equation (18) directly leads to the SINR on the lth layer

$$\gamma_l = \frac{\sigma_s^2}{\left(\sigma_n^2 + \sigma_{\mathrm{ICI}}^2 + \sigma_e^2\sigma_{\mathrm{d}}^2\right)\mathbf{e}_l^{\mathrm{H}}\left(\hat{\mathbf{G}}_{k,k}^{\mathrm{H}} \hat{\mathbf{G}}_{k,k}\right)^{-1}\mathbf{e}_l}. \tag{19}$$

Note that in practice variables $\sigma_s^2, \sigma_{\mathrm{d}}^2, \sigma_{\mathrm{ICI}}^2$, and σ_n^2 need to be replaced by their estimates.

Channel estimation

In this section, we present state-of-the-art channel estimators and derive analytical expressions for their MSE. Due to the orthogonal pilot symbol pattern utilized in LTE, the MIMO channel can be estimated as $N_{\mathrm{t}}N_{\mathrm{r}}$ individual SISO channels. To ease the reading, we thus simplify the notation in the following section and omit the antenna indices.

LS channel estimation

The LS channel estimate at the pilot symbol positions is obtained by solving the following minimization problem

$$\hat{\hat{\mathbf{H}}}_{\mathrm{p}}^{\mathrm{LS}} = \arg\min_{\hat{\hat{\mathbf{H}}}_{\mathrm{p}}} \left\|\mathbf{y}_{\mathrm{p}} - \hat{\hat{\mathbf{H}}}_{\mathrm{p}}\mathbf{x}_{\mathrm{p}}\right\|_2^2, \tag{20}$$

where the matrix $\hat{\hat{\mathbf{H}}}_{\mathrm{p}} \in \mathbb{C}^{N_{\mathrm{p}} \times N_{\mathrm{p}}}$ is assumed to be diagonal, representing the channel only at the pilot symbol positions. Obviously, such estimator ignores the non-diagonal elements in the channel matrix and treats the potential ICI as noise. More details on this topic can be found in [13]. The resulting MSE at the pilot symbol positions is given as

$$\sigma_{e_{\mathrm{p}}}^2 = \sigma_n^2 + \sigma_{\mathrm{ICI}}^2. \tag{21}$$

The channel estimates at the data positions have to be obtained using a two-dimensional interpolation. In this study, we restrict ourselves to a two-dimensional linear interpolation. At each data position, the three closest pilot symbols are located and the channel estimate is obtained by spanning a plane defined by the channel estimate at the closest pilot symbol's positions.

Figure 2 shows a channel estimate at 50 km/h of an LS estimator with a two-dimensional linear interpolation. The vertical lines represents pilot symbols. It can be observed, that the channel estimates at the data positions are obtained by spanning planes defined by the three nearest pilot symbols.

A channel estimate at an arbitrary data position using a linear interpolation is given by a weighted sum of the three nearest channel estimates (in the Euclidean sense of the time-frequency grid) at pilot positions, that span a plane.[b] Let us denote the channel estimate at the jth data position by $\hat{h}_{\mathrm{d},j}$ and the channel estimate at the ith pilot position by $\hat{h}_{\mathrm{p},i}$. Note that we use ith and jth positions as general description of location in the time-frequency grid:

$$\hat{h}_{\mathrm{d},j} = \sum_{i \in \mathcal{P}_j} w_{j,i}\hat{h}_{\mathrm{p},i}, \tag{22}$$

where $\mathcal{P}_j$ denotes a set of the three nearest pilot symbol positions to the data position j, that span a plane. The weight $w_{j,i}$ is a real number which implies how much the channel estimate at the jth data position is influenced by the channel estimate at the ith pilot position. The weight $w_{j,i}$ depends on the distance of the symbols in the time-frequency grid. The sum over $w_{j,i}$ over $i \in \mathcal{P}_j$ is one,

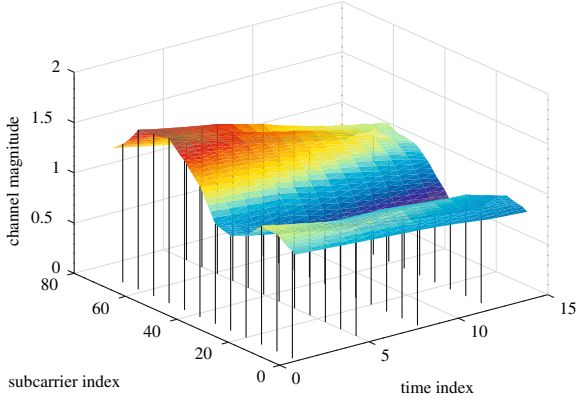

Figure 2 Linear interpolation of a channel at 50 km/h. Vertical lines represent positions of the pilot symbols.

namely $\sum_{i\in\mathcal{P}_j} w_{j,i} = 1$. Note that due to the linear interpolation/extrapolation by a plane, some weight can become negative.

It the following, we discuss how to obtain the weighting factor $w_{j,i}$ of Equation (22). First of all, we define a vector $\mathbf{p}_i$, whose entries are pilot positions of the ith pilot in the time-frequency grid, namely $\mathbf{p}_i = \left[f_i, t_i\right]^{\mathrm{T}}, i = 1, 2, \ldots, N_{\mathrm{p}}$, where the scalar f_i is a frequency index and t_i a time index. Similarly, we denote the position of the jth data symbol in the time-frequency grid by a vector $\mathbf{d}_j$.

Example. We assume that the channel of the first data symbol $h_{\mathrm{d},1}$ is located within the plane spanned by the channel estimates at the first three pilot symbols, $h_{\mathrm{p},1}$, $h_{\mathrm{p},2}$, and $h_{\mathrm{p},3}$. The plane spanned by these three channel estimates is defined as follows

$$\mathbf{d}_1 = \mathbf{p}_1 + a\left(\mathbf{p}_2 - \mathbf{p}_1\right) + b\left(\mathbf{p}_3 - \mathbf{p}_1\right), \tag{23}$$

where a and b are real scalars. For a general solution, Equation (23) can be reformulated as

$$\mathbf{d}_1 = (1 - a - b)\,\mathbf{p}_1 + a\mathbf{p}_2 + b\mathbf{p}_3. \tag{24}$$

Comparing Equation (22) with Equation (24), using a linear interpolation, we recognize that $w_{1,1} = 1 - a - b$, $w_{1,2} = a$, and $w_{1,3} = b$.

In the following, we evaluate the performance of such a channel estimator by analytically deriving its theoretical MSE at the data positions. Given the definition of the MSE

$$\begin{aligned}\sigma_e^2 &= \mathbb{E}\left\{\left\|h_{\mathrm{d},j} - \hat{h}_{\mathrm{d},j}\right\|^2\right\} \\ &= \mathbb{E}\left\{\left\|h_{\mathrm{d},j}\right\|^2\right\} - 2\Re\left\{\mathbb{E}\left\{h_{\mathrm{d},j}^{*}\hat{h}_{\mathrm{d},j}\right\}\right\} + \mathbb{E}\left\{\left\|\hat{h}_{\mathrm{d},j}\right\|^2\right\},\end{aligned} \tag{25}$$

let us analyze the three terms in Equation (25) individually. The first term is equal to one due to our system model $\mathbb{E}\left\{\left\|h_{\mathrm{d},j}\right\|^2\right\} = 1$. In the second term, $\hat{h}_{\mathrm{d},j}$ can be replaced by Equation (22)

$$\begin{aligned}\Re\left\{\mathbb{E}\left\{h_{\mathrm{d},j}^{*}\hat{h}_{\mathrm{d},j}\right\}\right\} &= \Re\left\{\mathbb{E}\left\{h_{\mathrm{d},j}^{*}\sum_{i\in\mathcal{P}_j} w_{j,i}\hat{h}_{\mathrm{p},i}\right\}\right\} \\ &= \Re\left\{\sum_{i\in\mathcal{P}_j} w_{j,i}\mathbb{E}\left\{h_{\mathrm{d},j}^{*}\left(h_{\mathrm{p},i} - n_{\mathrm{est},i}\right)\right\}\right\} \\ &= \sum_{i\in\mathcal{P}_j} w_{j,i}\Re\left\{R_{j,i}\right\}.\end{aligned} \tag{26}$$

The last step can be justified by the fact that the channel estimate at the pilot position can be represented as the true channel superimposed by some estimation error, and furthermore that this estimation error is uncorrelated with the channel value at the data position. The coefficient $R_{j,i} = \mathbb{E}\left\{h_{\mathrm{d},j}^{*}h_{\mathrm{p},i}\right\}$ denotes the correlation between the channels at the jth data symbol and the ith pilot symbol positions.

Let us proceed to the last term of Equation (25), in which we insert Equation (22) and consequently the equality $\hat{h}_{\mathrm{p},i} = h_{\mathrm{p},i} - n_{\mathrm{est},i}$, which states that the channel estimate at the pilot symbol position is given as the true channel superimposed by an estimation error. Note that due to Equation (8), it can be shown [1] that the MSE of the LS channel estimator at the pilot symbol positions is identical to the noise power σ_n^2 for time-invariant channels. In the case of time-variant channels, we have to consider also the ICI power. Therefore, the power of $n_{\mathrm{est},i}$ is equal to $\sigma_n^2 + \sigma_{\mathrm{ICI}}^2$. We obtain

$$\begin{aligned}\mathbb{E}\left\{\left\|\hat{h}_{\mathrm{d},j}\right\|^2\right\} &= \mathbb{E}\left\{\left\|\sum_{i\in\mathcal{P}_j} w_{j,i}\left(h_{\mathrm{p},i} - n_{\mathrm{est},i}\right)\right\|^2\right\} \\ &= \mathbb{E}\left\{\sum_{i\in\mathcal{P}_j}\sum_{i'\in\mathcal{P}_j} w_{j,i}w_{j,i'}\left(h_{\mathrm{p},i} - n_{\mathrm{est},i}\right)^{*}\right. \\ &\qquad \left.\times\left(h_{\mathrm{p},i'} - n_{\mathrm{est},i'}\right)\right\} \\ &= \sum_{i\in\mathcal{P}_j}\sum_{i'\in\mathcal{P}_j} w_{j,i}w_{j,i'}R_{i,i'} + \sum_{i\in\mathcal{P}_j} w_{j,i}^2\left(\sigma_n^2 + \sigma_{\mathrm{ICI}}^2\right).\end{aligned} \tag{27}$$

In the last step, we used the fact that the estimation error $n_{\mathrm{est},i}$ is statistically independent of the channel coefficients. To summarize, we obtain from Equation (25)

$$\begin{aligned}\sigma_e^2 &= \mathbb{E}\left\{\left\|h_{\mathrm{d},j} - \hat{h}_{\mathrm{d},j}\right\|^2\right\} \\ &= 1 - 2\sum_{i\in\mathcal{P}_j} w_{j,i}\Re\left\{R_{j,i}\right\} + \sum_{i\in\mathcal{P}_j}\sum_{i'\in\mathcal{P}_j} w_{j,i}w_{j,i'}R_{i,i'} \\ &\quad + \sum_{i\in\mathcal{P}_j} w_{j,i}^2(\sigma_n^2 + \sigma_{\mathrm{ICI}}^2).\end{aligned} \tag{28}$$

It is noticed that one part of Equation (28) is independent of $\sigma_n^2 + \sigma_{\mathrm{ICI}}^2$, as it only depends on the weights $w_{j,i}$ and the autocorrelation matrix. The dependency of the autocorrelation matrix can also be regarded as dependency on the maximum Doppler spread (or equivalently the user velocity). The second part of the MSE depends on $\sigma_n^2 + \sigma_{\mathrm{ICI}}^2$. This term is on the other hand independent of

the autocorrelation matrix. This can be stated analytically as follows

$$\sigma_e^2 = c_e\left(\sigma_n^2 + \sigma_{\mathrm{ICI}}^2\right) + d, \tag{29}$$

where c_e is a scalar depending on the weights $w_{j,i}$, given as

$$c_e = \frac{1}{N_\mathrm{d}} \sum_{j=1}^{N_\mathrm{d}} \sum_{i\in\mathcal{P}_j} w_{j,i}^2. \tag{30}$$

The value of c_e is obtained as arithmetical average over all data symbol positions. Its depends only on the pilot symbols pattern. In case of a two-dimensional linear interpolation with LTE pilot symbol pattern using an LS channel estimator, we find $c_e = 0.6623$ evaluating Equation (30). The constant d is a scalar depending on the weights $w_{j,i}$ as well as the autocorrelation matrix. In the following text, it is referred to as channel saturation d, given as

$$d = \frac{1}{N_\mathrm{d}} \sum_{j=1}^{N_\mathrm{d}} \left(1 - 2\sum_{i\in\mathcal{P}_j} w_{j,i}\Re\left\{R_{j,i}\right\} + \sum_{i\in\mathcal{P}_j}\sum_{i'\in\mathcal{P}_j} w_{j,i}w_{j,i'}R_{i,i'}\right). \tag{31}$$

Figure 3 shows the value of the channel saturation coefficient d over user velocity for different antenna configurations. Its value grows with increasing user velocity. Note that the channel saturation coefficient d in Equation (29) causes the error floor in the MSE of the LS channel estimator. This saturation originates from a low correlation over time. Figure 4 shows the simulated and theoretical MSE of an LS channel estimator. An excellent agreement can be found.

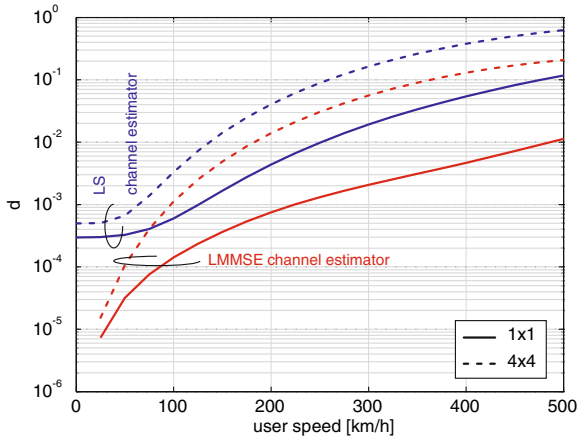

Figure 3 Channel saturation coefficient *d* plotted over user velocity for a different number of transmit antennas. This parameter is the same for one and two transmit antennas.

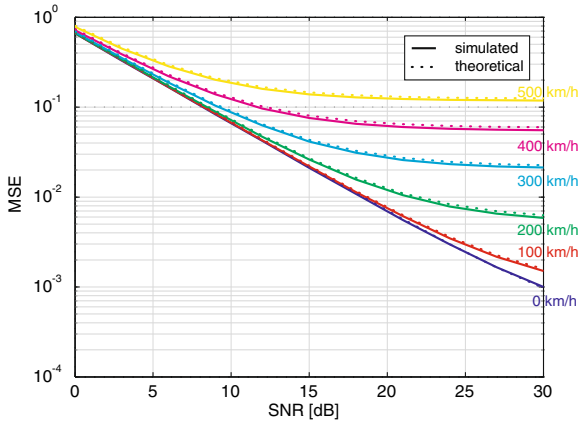

Figure 4 Comparison between theoretical and simulated MSE of an LS channel estimator for 1 × 1 system at different user velocities.

LMMSE channel estimation

The LMMSE channel estimator requires knowledge of the second-order statistics of the channel and the noise. It can be shown that the LMMSE channel estimate is obtained by multiplying the LS estimate with a filtering matrix $\mathbf{A}_{\mathrm{LMMSE}} \in \mathbb{C}^{N_\mathrm{d}\times N_\mathrm{p}}$ [14]

$$\hat{\mathbf{h}}_\mathrm{d}^{\mathrm{LMMSE}} = \mathbf{A}_{\mathrm{LMMSE}}\hat{\mathbf{h}}_\mathrm{p}^{\mathrm{LS}}. \tag{32}$$

In order to find the LMMSE filtering matrix, the MSE

$$\sigma_e^2 = \mathbb{E}\left\{\left\|\mathbf{h}_\mathrm{d} - \mathbf{A}_{\mathrm{LMMSE}}\hat{\mathbf{h}}_\mathrm{p}^{\mathrm{LS}}\right\|_2^2\right\}, \tag{33}$$

has to be minimized, leading to

$$\mathbf{A}_{\mathrm{LMMSE}} = \mathbf{R}_{\mathbf{h}_\mathrm{d},\mathbf{h}_\mathrm{p}}\left(\mathbf{R}_{\mathbf{h}_\mathrm{p},\mathbf{h}_\mathrm{p}} + \left(\sigma_n^2 + \sigma_{\mathrm{ICI}}^2\right)\mathbf{I}\right)^{-1}, \tag{34}$$

where the matrix $\mathbf{R}_{\mathbf{h}_\mathrm{p},\mathbf{h}_\mathrm{p}} = \mathbb{E}\left\{\mathbf{h}_\mathrm{p}\mathbf{h}_\mathrm{p}^\mathrm{H}\right\} \in \mathbb{C}^{N_\mathrm{p}\times N_\mathrm{p}}$ denotes the channel autocorrelation matrix at the pilot symbols, and the matrix $\mathbf{R}_{\mathbf{h}_\mathrm{d},\mathbf{h}_\mathrm{p}} = \mathbb{E}\left\{\mathbf{h}_\mathrm{d}\mathbf{h}_\mathrm{p}^\mathrm{H}\right\} \in \mathbb{C}^{N_\mathrm{d}\times N_\mathrm{p}}$ is the channel cross-correlation matrix.

To derive the theoretical MSE, we plug Equation (34) into Equation (33):

$$\begin{aligned}\sigma_e^2 =& \mathbb{E}\left\{\left(\mathbf{h}_\mathrm{d} - (\mathbf{R}_{\mathbf{h}_\mathrm{d}},\mathbf{h}_\mathrm{p}(\mathbf{R}_{\mathbf{h}_\mathrm{p}},\mathbf{h}_\mathrm{p} - \left(\sigma_n^2 + \sigma_{\mathrm{ICI}}^2\right)\mathbf{I})^{-1}\hat{\mathbf{h}}_\mathrm{p}^{\mathrm{LS}}\right)\right.\\ &\left.\times\left(\mathbf{h}_\mathrm{d} - (\mathbf{R}_{\mathbf{h}_\mathrm{d},\mathbf{h}_\mathrm{p}}(\mathbf{R}_{\mathbf{h}_\mathrm{p},\mathbf{h}_\mathrm{p}} - \left(\sigma_n^2 + \sigma_{\mathrm{ICI}}^2\right)\mathbf{I})^{-1}\hat{\mathbf{h}}_\mathrm{p}^{\mathrm{LS}}\right)\right)^\mathrm{H}\right\}\end{aligned} \tag{35}$$

After a straightforward manipulation, the average MSE at the data subcarriers is expressed as

$$\sigma_e^2 = \frac{1}{N_\mathrm{d}}\mathrm{tr}\left\{\mathbf{R}_{\mathbf{h}_\mathrm{d},\mathbf{h}_\mathrm{d}} - \mathbf{R}_{\mathbf{h}_\mathrm{d},\mathbf{h}_\mathrm{p}}\left(\mathbf{R}_{\mathbf{h}_\mathrm{p},\mathbf{h}_\mathrm{p}} + \left(\sigma_n^2 + \sigma_{\mathrm{ICI}}^2\right)\mathbf{I}\right)^{-1}\mathbf{R}_{\mathbf{h}_\mathrm{p},\mathbf{h}_\mathrm{d}}\right\}, \tag{36}$$

where N_d is the number of data symbols. Figure 5 depicts the simulated (solid line) and the analytical (dashed line)

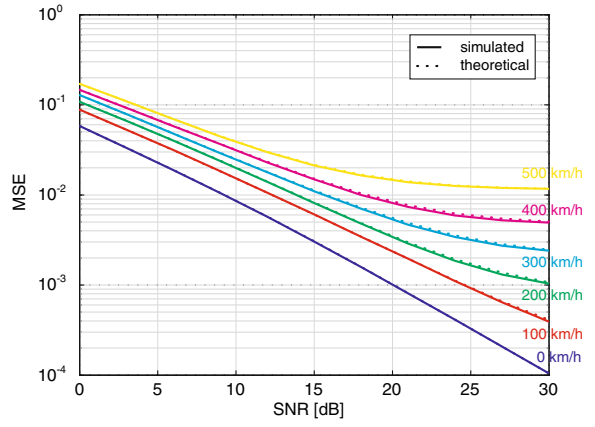

Figure 5 Comparison between theoretical and simulated MSE of an LMMSE channel estimator for 1 × 1 system at different user velocities.

MSE of an LMMSE channel estimator at different user velocities. The simulated MSE and the analytically derived MSE show nearly perfect identity. Considering this figure, it may be believed that a similar decomposition is possible as in the case of an LS channel estimator. However, this is not the case. The MSE of an LMMSE channel estimator can only be approximated by

$$\sigma_e^2 \approx c_e \left(\sigma_n^2 + \sigma_{\mathrm{ICI}}^2\right) + d, \tag{37}$$

where the scalar coefficient c_e and the channel saturation coefficient d can be obtained by the following method. Let us assume that there is no noise and insert $\sigma_n^2 = 0$ and $\sigma_{\mathrm{ICI}}^2 = 0$ into Equation (36), providing us with an MSE value for infinitely high SNR, i.e., in the point of the MSE saturation. Such saturation is expressed by the value of d. Figure 3 shows the value of the channel saturation coefficient d over user velocity for 1×1 and 4×4 systems for LTE pilot symbol pattern. In case of a 2×2 system using the pilot symbol pattern defined in LTE, the channel saturation coefficient d is the same as in a 1×1 case, since the amount of the pilot symbols is the same and an LMMSE estimator performs identically. The value of c_e can be obtained by calculating the true MSE and solving $\sigma_e^2 = c_e \left(\sigma_n^2 + \sigma_{\mathrm{ICI}}^2\right) + d$.

Power allocation

In this section, we analytically derive an optimal power distribution among pilot and data symbols in high velocity scenarios. As a cost function, we choose the post-equalization SINR in Equation (19). Although the provided results are shown in the context of the current LTE standard, the presented concept can be applied to any MIMO OFDM-based system.

We introduce power adjusting factors c_{p}^2 and c_{d}^2 for the pilot and data symbols, respectively. Since the overall transmit power remains constant, that can be expressed by

$$c_{\mathrm{p}}^2 N_{\mathrm{p}} + c_{\mathrm{d}}^2 N_{\mathrm{d}} = N_{\mathrm{p}} + N_{\mathrm{d}}, \tag{38}$$

where N_{p} and N_{d} represent the number of pilot symbols and data symbols in a subframe, respectively. In order to describe the interconnection between c_{p}^2 and c_{d}^2, we introduce a variable p_{off} which is the power offset between the power of the pilot symbols and the data symbols, denoted by

$$c_{\mathrm{d}}^2 = p_{\mathrm{off}} c_{\mathrm{p}}^2. \tag{39}$$

Therefore, c_{p}^2 and c_{d}^2 can be expressed with respect to p_{off}:

$$c_{\mathrm{p}}^2 = \frac{N_{\mathrm{p}} + N_{\mathrm{d}}}{p_{\mathrm{off}} N_{\mathrm{d}} + N_{\mathrm{p}}}, \tag{40}$$

$$c_{\mathrm{d}}^2 = \frac{N_{\mathrm{p}} + N_{\mathrm{d}}}{N_{\mathrm{d}} + \frac{N_{\mathrm{p}}}{p_{\mathrm{off}}}} = p_{\mathrm{off}} c_{\mathrm{p}}^2. \tag{41}$$

For the aforementioned channel estimators, we increase the power at the pilot symbol by c_{p}^2, the noise and ICI-dependent parts of the MSEs in Equation (29) and (37) decrease by the same factor c_{p}^2. Therefore, we have

$$\tilde{\sigma}_e^2 = c_e \frac{\left(\sigma_n^2 + \sigma_{\mathrm{ICI}}^2\right)}{c_{\mathrm{p}}^2} + d. \tag{42}$$

Plugging the variables c_{d}^2 and c_{p}^2 into Equation (19), we obtain the SINR expression at layer l with adjusted power of the pilot symbols

$$\gamma_l = \frac{\sigma_s^2 c_{\mathrm{d}}^2}{\left(\sigma_n^2 + \sigma_{\mathrm{ICI}}^2 + \tilde{\sigma}_e^2 \sigma_{\mathrm{d}}^2 c_{\mathrm{d}}^2\right) \mathbf{e}_l^{\mathrm{H}} \left(\mathbf{G}^{\mathrm{H}} \mathbf{G}\right)^{-1} \mathbf{e}_l}. \tag{43}$$

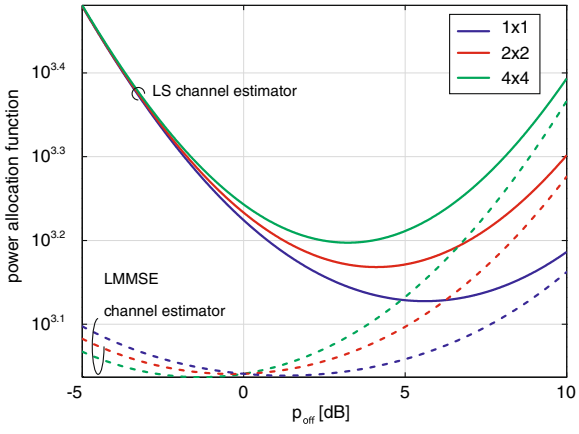

Figure 6 Power allocation function $f(p_{\mathrm{off}})$ for different antenna configurations.

Table 2 Values of the parameters of $f(p_{\text{off}})$ for different number of transmit antennas for 1.4 MHz bandwidth, ITU PedA[16] channel model, LS, and LMMSE channel estimators

Parameter	Tx = 1	Tx = 2	Tx = 4
N_{d}	960	912	864
N_{p}	48	96	144
LS			
c_e	0.6623	0.6971	0.7359
$p_{\text{off,opt}}$ (dB)	≈5.61	≈4.11	≈3.22
LMMSE			
$p_{\text{off,opt}}$ (dB)	≈1.27	≈-0.35	≈-1.35

Insert Equation (40) and Equation (41) into Equation (43) and simplify the expression, we obtain the SINR expression as a function of p_{off}:

$$\gamma_l = \frac{1}{\frac{N_{\text{l}}(\sigma_n^2+\sigma_{\text{ICI}}^2)\mathbf{e}_l^{\text{H}}(\mathbf{G}^{\text{H}}\mathbf{G})^{-1}\mathbf{e}_l}{N_{\text{d}}+N_{\text{p}}}\left(f\left(p_{\text{off}}\right)+\tilde{d}\right)}, \tag{44}$$

for which the power allocation function $f(p_{\text{off}})$ is given as

$$f(p_{\text{off}}) = \left(p_{\text{off}}N_{\text{d}} + N_{\text{p}}\right)\left(\frac{1}{p_{\text{off}}} + c_e\right). \tag{45}$$

The constant $\tilde{d}$ is proportional to the channel saturation coefficient d and is given as

$$\tilde{d} = d\frac{N_{\text{p}} + N_{\text{d}}}{\sigma_n^2 + \sigma_{\text{ICI}}^2}. \tag{46}$$

Note that Equation (45) is independent of channel realization, noise variance, ICI power and even user velocity. It is the same as in [1], only the constant c_e has a different value due to the distinct performance of the channel estimators. Let us focus on the term $\tilde{d}$ in Equation (44). This term is always positive. It thus becomes obvious that it causes the overall limitation of the post-equalization SINR. Even if the power allocation function would be very small, the expression in the brackets of the denominator in Equation (44) will not be smaller than the value of $\tilde{d}$. This term is dependent on the noise variance, ICI power and the factor d, which is dependent on the user velocity. This term not only causes limitations in terms of post-equalization SINR, but when it becomes larger than the power allocation function, it also causes the post-equalization to be less sensitive to the variable p_{off}.

Before, we find the minimum of the power allocation function, let us discuss the expected solution. Intuitively, we would expect that once we have reached the saturation in the MSE of a channel estimator, it does not pay off to increase the power radiated at the pilot symbols, since the MSE will not become better. However, consider for a moment Equation (43), especially the term $\tilde{\sigma}_e^2\sigma_{\text{d}}^2c_{\text{d}}^2$ that corresponds to the interlayer interference caused by the channel estimation error. By increasing the power radiated at the data symbols, the interlayer interference is also increased. Therefore, even if the saturation of a channel estimator is reached, it might not be beneficial to decrease the power radiated at the pilot symbols [15].

Let us proceed to the definition of the optimization problem. The target is to find an optimal value of $p_{\text{off,opt}}$ that maximizes the post-equalization SINR while keeping the overall transmit power constant

$$\begin{aligned} &\underset{p_{\text{off}}}{\text{maximize}} && \gamma_l \\ &\text{subject to} && N_{\text{d}}c_{\text{d}}^2\sigma_{\text{d}}^2 + N_{\text{p}}c_{\text{p}}^2\sigma_{\text{p}}^2 = N_{\text{d}} + N_{\text{p}} \end{aligned} \tag{47}$$

In order to maximize the post-equalization SINR, the power allocation function $f(p_{\text{off}})$ in the denominator of Equation (44) has to be minimized. The minimum of the power allocation function $f(p_{\text{off}})$ can be found by simple differentiation, resulting in

$$p_{\text{off,opt}} = \sqrt{\frac{N_{\text{p}}}{N_{\text{d}}c_e}}. \tag{48}$$

Figure 6 shows an example of the power allocation function for LS and LMMSE channel estimators for various numbers of transmit antennas. We observe, that

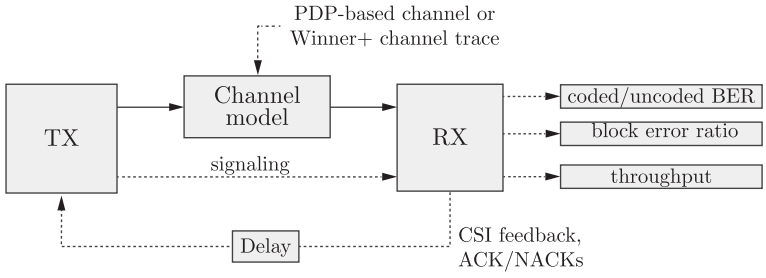

Figure 7 Structure of the Vienna LTE Link Level Simulator.

all of these functions have minimum points. This minimum point corresponds to the maximization of the post-equalization SINR. Typical values of parameters N_d, N_p, and c_e are provided in Table 2. Note, that although N_d and N_p depend on the utilized bandwidth, the minimum of $f(p_{off})$ is independent of it, since N_d and N_p scale with the same constant with increasing bandwidth and actually only their ratio is what matters. The value of c_e is different for four transmit antennas due to the lower number of pilot symbols at the third and fourth antennas. The last row of Table 2 presents the optimal values of $p_{off,opt}$ for different numbers of transmit antennas and an ITU VehA [16] type channel model.

Simulation results

In this section, we present simulation results and discuss the performance of LTE transmission systems with different pilot symbol powers under time-variant channels. All results are obtained with the LTE Link Level Simulator version "r1089" [8,9], which can be downloaded from www.nt.tuwien.ac.at/ltesimulator. All data, tools, and scripts are available online [17] in order to allow other researchers to reproduce the results shown in this article. The structure of the utilized Vienna LTE Link Level simulator is shown in Figure 7. Note that the simulator performs all routines according to the standard [10] and it includes blocks like frequency offset compensation [18], timing offset compensation [19], channel estimation [13], and more.

Conclusion

Table 3 presents the most important simulator settings. Since what is to be observed is the optimal value of pilot symbol power adjustment, an SNR of 10 dB has been chosen.

Simulation results showing throughput performance for 1×1, 2×2, and 4×4 antenna configurations are shown in Figure 8 for LS and LMMSE channel estimators. In this example, we set the user velocity to 100 km/h and SNR = 10 dB. Little arrows always indicate the theoretically derived optimal value of the variable p_{off}, that maximizes the post-equalization SINR. Detailed values

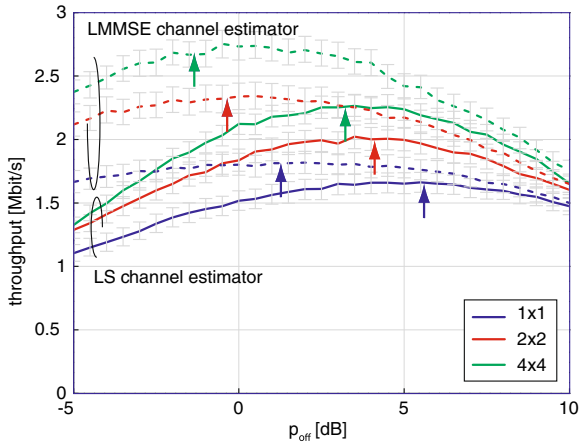

Figure 8 Throughput curve of LTE system over p_{off} using different channel estimators and various antenna setups. Little arrows always indicate the theoretically derived optimal value of the variable p_{off}, that maximizes the post-equalization SINR.

are listed in Table 2. The simulation results show an excellent match with the analytical solution shown in Section "Power allocation". Using the optimal value of power offsets between pilot and data symbols results in throughput maximization. Moving away from this value, a throughput loss can be observed. However, this loss is usually not severe and the relatively broad maximum indicates a high robustness against inaccurate power distribution between pilot and data symbols.

A negative value of the variable p_{off} (in dB) corresponds to the reduction of the power radiated at the pilot symbols and increasing power radiated at the data symbols. Such negative value is optimal in case of four transmit antennas applying an LMMSE estimator. This kind of channel estimator is of superb performance and therefore requires less power to obtain a high-quality channel estimate.

Considering a single transmit antenna with an LS channel estimator, the optimal value of $p_{off,opt} = 5.61$ dB may be considered rather high. However, due to the low number of pilot symbols compared to the number of data

Table 3 Simulator settings for fast fading simulations

Parameter	Value
Bandwidth	1.4 MHz
Number of transmit antennas	1, 2, 4
Number of receive antennas	1, 2, 4
Receiver type	ZF
Transmission mode	Open-loop spatial multiplexing
Channel type	ITU VehA [16]
MCS	Adaptive

Table 4 Throughput gain when using optimal power distribution between data and pilot symbols for various number of transmit antennas and LS and LMMSE channel estimators

Parameter	Tx = 1	Tx = 2	Tx = 4
LS			
Throughput gain	10%	10%	7%
LMMSE			
Throughput gain	0.5%	0.1%	0.7%

symbols, the difference in terms of energy is much lower than in terms of power.

An OFDM transmission system that does not utilize different power levels for its pilot and data symbols, corresponds to $p_{\text{off}} = 0$ dB. In Figure 8, we observe that using optimal power distribution results in throughput gains up to 10%. Table 4 summarizes throughput gain in percent of a system using optimal power distribution between data and pilot symbols compared to one that does not. For the LMMSE channel estimators, only a small gain can be observed because the values of $p_{\text{off,opt}}$ are close to 1 (0 dB). Therefore, a system with equal power radiated at the pilot and data symbols is already close to optimal.

In this article, we answer the question of how to distribute power between pilot and data symbols in a way, that maximizes the overall performance of an OFDM MIMO system under time-variant channels. For this purpose, we made use of the post-equalization SINR with imperfect channel knowledge. Furthermore, we generalized the solution to the power distribution problem for time-variant channels. Simulation results obtained by the Vienna LTE simulator confirm our analytical solution. We also provide scripts, that allow to reproduce all results shown in this article. By adjusting the pilot symbol power individually, the solution from this article allows to increase the throughput of a transmission system by up to 10%.

Endnotes

[a]We are devoted to provide reproducible results. Thus, following our previous work, all data, tools, as well implementations needed to reproduce the results of this article can be downloaded from our homepage [17].

[b]Note that the three nearest pilot symbols cannot be located on the same subcarrier or within the same OFDM symbol. Would it be the case, they would not span any plane. In LTE, this is not of concern due to the defined pilot symbol pattern.

Competing interests
The authors declare that they have no competing interests.

Acknowledgements
The authors would like to thank the LTE research group and in particular Prof. Christoph Mecklenbräuker and Prof. Paulo S. R. Diniz for continuous support and lively discussions. This study was funded by the Christian Doppler Laboratory for Wireless Technologies for Sustainable Mobility, KATHREIN-Werke KG, and A1 Telekom Austria AG. The financial support by the Federal Ministry of Economy, Family and Youth and the National Foundation for Research, Technology and Development is gratefully acknowledged.

Received: 15 February 2012 Accepted: 12 June 2012
Published: 20 July 2012

References

1. M Šimko, S Pendl, S Schwarz, Q Wang, JC Ikuno, M Rupp, in *Proc. 74th IEEE Vehicular Technology Conference (VTC2011-Fall),* Optimal pilot symbol power allocation in LTE, San Francisco, USA, 2011
2. C Novak, G Matz, in *Proc. of SPAWC 2010,* Low-complexity MIMO-BICM receivers with imperfect channel state information: capacity-based performance comparison, Marrakech (Morocco), 2010
3. E Alsusa, MW Baidas, Y Lee, in *Proc. of IEEE PIMRC 2005,* vol. 1, On the impact of efficient power allocation in pilot based channel, estimation techniques for multicarrier systems. (2005), pp. 706–710
4. J Chen, Y Tang, S Li, *Pilot power allocation for OFDM systems*. (2003), pp. 1283–1287
5. B Hassibi, B Hochwald, How much training is needed in multiple-antenna wireless links? IEEE Trans. Inf. Theory. **49**(4), 951–963 (2003)
6. J Wang, OY Wen, H Chen, S Li, Power allocation between pilot and data symbols for MIMO systems with MMSE detection under MMSE channel estimation, EURASIP J. Wirel. Commun. Netw (2011)
7. M Šimko, M Rupp, in *Conference Record of the Fourtyfifth Asilomar Conference on Signals, Systems and Computers, 2011,* Optimal pilot symbol power allocation in multi-cell scenarios of LTE, Pacific Grove, USA, 2011
8. C Mehlführer, M Wrulich, JC Ikuno, D Bosanska, M Rupp, in *Proc. of EUSIPCO 2009,* Simulating the long term evolution physical layer, Glasgow, Scotland, 2009
9. C Mehlführer, JC Ikuno, M Šimko, S Schwarz, M Wrulich, M Rupp, The Vienna LTE Simulators—enabling reproducibility in wireless communications research, EURASIP J. Adv. Signal Process. **2011**, 1–13 (2011)
10. 3GPPm, Evolved Universal Terrestrial Radio Access (E-UTRA); Physical channels and modulation. TS 36.211, 3rd Generation Partnership Project (3GPP) (2008), http://www.3gpp.org/ftp/Specs/html-info/36211.htm
11. A Hedayat, A Nosratinia, N Al-Dhahir, in *Proc. of IEEE ICASSP 2005,* vol. 3, Linear equalizers for flat rayleigh MIMO channels. (2005), pp. iii/445–iii/448
12. Y Li, LJ Cimini, Bounds on the interchannel interference of OFDM in time-varying impairments, IEEE Trans. Commun. **49**(3), 401–404 (2001)
13. M Šimko, C Mehlführer, M Wrulich, M Rupp, in *Proc. of WSA 2010,* Doubly dispersive channel estimation with scalable complexity, Bremen, Germany, 2010
14. S Omar, A Ancora, D Slock, in *Proc. of IEEE PIMRC 2008,* Performance analysis of general pilot-aided linear channel estimation in LTE OFDMA systems with application to simplified MMSE schemes. (2008), pp, 1–6
15. M Šimko, PSR Diniz, Q Wang, M Rupp, in *Proc. 76th IEEE Vehicular Technology Conference (VTC2011-Fall),* Power efficient pilot symbol power allocation under time-variant channels, Quebec, Canada, 2012
16. ITU: Recommendation ITU-R M.1225: Guidelines for Evaluation of Radio Transmission Technologies for IMT- 2000 Systems. Recommendation ITU-R M.1225, International Telecommunication Union, 1998
17. LTE simulator homepage, online, http://www.nt.tuwien.ac.at/ltesimulator/
18. Q Wang, M Rupp, in *Conference Record of the Fourtyfifth Asilomar Conference on Signals, Systems and Computers, 2011 (Asilomar-2011),* Analytical link performance evaluation of LTE downlink with carrier frequency offset, Pacific Grove, USA, 2011
19. Q Wang, M Šimko, M Rupp, in *IEEE Proceedings of Workshop on Smart Antennas 2012 (WSA-2012),* Performance analysis of LTE downlink under symbol timing offset, Dresden, Germany, 2012

doi:10.1186/1687-1499-2012-225
Cite this article as: Simko *et al.*: Optimal pilot symbol power allocation under time-variant channels. *EURASIP Journal on Wireless Communications and Networking* 2012 **2012**:225.